


 Cite this: *RSC Adv.*, 2022, **12**, 8691

# Wearable microfluidic-based e-skin sweat sensors

 Humairah Tabasum,<sup>†ab</sup> Nikita Gill,<sup>†ab</sup> Rahul Mishra<sup>†ab</sup> and Saifullah Lone <sup>\*ab</sup>

Electronic skins (e-skins) are soft (deformable and stretchable) state-of-the-art wearable devices that emulate the attributes of human skin and act as a Human–Machine Interface (HMI). Recent advances in e-skin for real-time detection of medical signals such as pulse, temperature, electromyogram (EMG), electroencephalogram (EEG), electrooculogram (EOG), electrocardiogram (ECG), and other bioelectric signals laid down an intelligent foundation for early prediction and diagnosis of diseases with a motive of reducing the risk of the ailment reaching to the end stage. In particular, sweat testing has been employed in diverse applications ranging from medical diagnosis of diabetes, cystic fibrosis, tuberculosis, blood pressure, and autonomic neuropathy to evaluating fluid and electrolyte balance in athletes. Typically, sweat testing techniques are done by trained experts and require off-body measurements, which prevent individuals from de-coding health issues quickly and independently. With the onset of soft electronics, wearable sweat sensors overcome this disadvantage *via in situ* sweat measurements with real-time feedback, timely diagnosis, creating the potential for preventive care and treatment. Over the past few decades, wearable microfluidic-based e-skin sweat sensors have paved a new way, promising sensing interfaces that are highly compatible with arranging medical and electronic applications. The present review highlights the recent research carried out in the microfluidic-based wearable sweat sensors with a critical focus on real-time sensing of lactate, chloride, and glucose concentration; sweat rate, simultaneously with pH, and total sweat loss for preventive care, timely diagnosis, and point-of-care health and fitness monitoring.

 Received 26th October 2021  
 Accepted 27th February 2022

DOI: 10.1039/d1ra07888g

[rsc.li/rsc-advances](http://rsc.li/rsc-advances)

## 1. Introduction

Melanie Walker (Co-chair, Future Council, World Economic Forum) predicted hospitals could be a thing of the past in just

over a decade.<sup>1</sup> Hospitals would be replaced by decentralized disruptive mobile and wearable technologies for efficient and cost-effective healthcare services.<sup>1</sup> Due to their wide-spectrum diagnostic and disease monitoring applications, the development of robust skin mimicking technologies with superior real-time sensing characteristics has grabbed tremendous attention from both industry and academia.<sup>2–4</sup> In this regard, significant efforts have been made towards realizing the scope of electronic skins (*i.e.*, e-skins) with superior sensory capabilities.<sup>5–8</sup> The demand for wearable biosensors is ambitious for a personalized

<sup>a</sup>Department of Chemistry, National Institute of Technology (NIT), Srinagar, J&K, India, 190006. E-mail: saifullah.lone@nitsri.net; Tel: +91-60005221589

<sup>b</sup>iDREAM (Interdisciplinary Division for Renewable Energy & Advanced Materials), NIT, Srinagar, India, 190006

<sup>†</sup> These authors contributed equally.



*Humairah Tabasum is currently a master's student in the Department of Chemistry, National Institute of Technology (NIT) Srinagar, Jammu and Kashmir, India. In 2020, she obtained her undergraduate degree in basic science from the University of Kashmir, India. Her research interests are Soft Materials, Nanochemistry, and Computational Chemistry.*



*Nikita Gill is currently a master's student in the Department of Chemistry, National Institute of Technology (NIT) Srinagar, Jammu and Kashmir, India. She received her undergraduate degree in basic science from the Chaudhary Ranbir Singh University, Haryana, in 2020. Her research interests are Nanochemistry, Biosensors, and Material Chemistry.*



health care system—that could constantly monitor chronically ill elderly patients and evaluate the physical and chemical biomarkers in an athlete's sweat.<sup>3–5</sup> Ever since, sweat was known to be excreted from the skin at elevated body temperature, it has been exploited to examine various diseases of critical concern.<sup>9–11</sup> Sweat is a non-invasively collectible bio-fluid comprising a range of electrolytes, proteins, and lipids of particular interest in diagnosing various diseases.<sup>12,13</sup> As a result, sweat hosts a vital panel of biomarkers to reveal essential information about a person's metabolic state.<sup>11,14,15</sup> Furthermore, sweat biochemical analysis is a promising method for monitoring continuous health states for example, hydration status, drug personalization, cystic fibrosis, tuberculosis, and diabetes diagnosis.<sup>16,17</sup>

The development of wearable biosensors based on textile materials, skin patches, and contact lenses is used for the noninvasive continuous monitoring of various diseases.<sup>18</sup> Therefore, there is an overwhelming scope for soft material-based implanted wearable sensors in clinical diagnostics. Soft material-based wearable biosensors are highly desirable because of their softness, compatibility, elasticity, and extensibility.<sup>19–21</sup> Such biosensors are easy to use and reduce tissue damage.<sup>1,22</sup>

In this view, tremendous efforts have been made to collect and detect sweat by implicating the direct connection of sensors and skin. The sensors, such as fabric/or paper substrates and temporary tattoos, collect the sweat—for electrochemical analysis/or optical assessment.<sup>23</sup> Sensors are directly laminated onto the skin epidermis for real-time sensing of chemical components such as chloride ( $\text{Cl}^-$ ) ions, sodium ( $\text{Na}^+$ ) ions, and lactate.<sup>24–26</sup> Real-time sweat analysis in functionalized porous films could produce valuable chemical information including sweat pH *via* colourimetric responses. Also, they allow

quantitative tests by employing smartphone devices to collect high-quality digital photos for data analysis.<sup>27,28</sup> Mechanical signal sensing is essential for e-skin sensors to detect pressures and strains, which provides haptic interactions with electronic devices, human action feedback, and health monitoring.<sup>29–31</sup>

Lately, the introduction of microfluidics into mechanical sensing has broadened the application spectrum of the field—given the easy, scalable, environmentally friendly manufacturing and the remarkable adaptation of microfluidic-based sensors to complicated target forms.<sup>32–35</sup> In this regard, some thin/or softly closed miniature microfluidic-based sensors could directly obtain sweat from pores on the skin's surface—for quick investigation.<sup>27</sup> The microfluidic systems collect sweat from a variety of channels, and have the option of wirelessly connecting to external devices for image capturing and analysis, as well as for multi-parametric sensing of markers of clinical value.<sup>36</sup> This type of microfluidic technology, which incorporates fluid handling and capture and biochemical analytical functionality, builds on recently reported epidermal electronic, photonic, and optoelectronic systems.<sup>37–39</sup> It is possible to implant microfluidic devices in various locations on the body without causing chemical/or physical discomfort due to biocompatible adhesives and soft device mechanics (including flexible and elastic characteristics and watertight interfaces).<sup>36</sup> Employing wireless data transmission instruments could quantify total sweat loss and the concentration of pH, lactate, chloride, and glucose.<sup>36,40,41</sup> Thus, due to their cost-effective, industrial scale, and eco-friendly fabrication approach, microfluidics-based health monitoring devices offer wide-spectrum applications in sweat sensing. Furthermore, wearable microfluidics-based sweat sensors are more attractive and scientifically desirable given their excellent adaptability to the



*Rahul Mishra is currently a master's student in the Department of Chemistry, National Institute of Technology (NIT) Srinagar, Jammu and Kashmir, India. He pursued an undergraduate degree in basic science from Sambalpur University, Odisha, in 2020. His research interests are Nanotechnology, Solid-state Chemistry, and Electrochemistry.*



*Saifullah Lone, PhD Dr Saifullah Lone attained Bachelor's and Master's degrees in Chemistry from Aligarh Muslim University (AMU), India. He pursued PhD in Droplet Microfluidics from the Department of Applied Chemistry, Kyungpook National University (KNU), South Korea, in 2012. After PhD, Dr Lone worked with various universities, including—Seoul National University (SNU), King*

*Abdullah University of Science & Technology (KAUST), Kyungpook National University (KNU), and Pusan National University (PNU) as a Foreign Researcher, Postdoctoral Fellow and Research Professor. He is currently a Principal Investigator at Interdisciplinary Division for Renewable Energy and Advanced Materials (iDREAM), Department of Chemistry, National Institute of Technology (NIT), Srinagar, India. His research interests are Soft Materials, Microfluidics, Soft Actuators, Solid-Liquid Interface, & Bioinspired Materials.*





Fig. 1 Scheme representation of microfluidic-base e-Skin sensors in tracking human health.

complex target shapes and their facile integration with other biological sensors and surfaces.<sup>32–35</sup>

Unlike the other review articles highlighting wearable biosensors produced by expensive and time-consuming techniques with delayed, slow responses towards monitoring various diseases.<sup>42–45</sup> The review mainly tracks the latest scientific knowledge and state-of-the-art microfluidic-based wearable sweat sensors for quick/or precise analysis, diagnosis, and monitoring of sweat-linked abnormalities. The novelty of review is in highlighting the microfluidic-based soft e-Skin sweat sensors—which are; (a) easy to laminate onto skin at different angles/or curvatures, (b) follow simple fluidic principles in operation, (c) easy to fabricate at industrial scale, and (d) cost-effective for general public. Furthermore, recent applications of microfluidic-based wearable sensors for human health monitoring applications are included. Finally, we discuss the current challenges with microfluidic-based wearable sensors and the possible solutions. The schematic representation of microfluidic-base e-Skin sensors with applications in various critical areas of human health is highlighted in the Fig. 1.

## 2. Electrochemical principle of sweat sensing

In general, sensing is dependent on the signal transduction process. Sweat sensing requires a quick response, *in situ*

processing, and precise monitoring input. In this regard, optical and colorimetric techniques have been explored to be useful in certain applications. However, when these techniques are deployed for point-of-care bio-fluid analysis, they show certain limitations (Table 1). On the other hand, the electrochemical technologies provide substantial advantages in advanced bio-fluid monitoring systems due to their quick reaction, high sensitivity, and selectivity, as well as their low cost.<sup>20,46–48</sup> While certain complicated calibrations are required, electrochemical sweat sensors are capable of operating with small sample amounts and providing rapid, real-time, and continuous responses. A comprehensive electrochemical sweat sensor is made up of three critical components that each performs a unique function: a microfluidic device, a sensing system, and an electrical component. To begin, a microfluidic device transports sweat from the skin to the sensor region in a continuous fashion. The sensing structure is implemented of an array of distinct functional electrodes that are capable of rapidly converting analyte concentrations to electrical signals. Following that, the associated electronic component would process, calibrate, and transmit the resulting electrical signals for reading. In contrast to the relatively standardized procedures of electrical signal processing and calibration, each electrochemical signal is generated using a unique sensing material and mechanism. The sweat components, concentrations, and electrochemical sensing mode are summarized in Table 2. To construct target sweat sensors, it is critical to have



Table 1 Analytes and analytical techniques employed in sweat analyzers

Sensing techniques	Advantages	Disadvantages
Electrochemistry	Highly sensitive and selective, rapid, real-time, and continuous response, may operate with tiny amounts of bio-fluid and detect biomarker concentrations as low as 0.1 ng mL <sup>-1</sup>	Complex data calibration
Colorimetry	Selective, simple to use, visually appealing, and easily readable with the naked eye	Cannot obtain a continuous response; significantly impacted by sweat turbidity; requires advanced devices capable of obtaining high-quality digital pictures to do quantitative analysis
Optic	Rapid reaction, selectivity, ability to detect and monitor tiny volumes online, immunity to electromagnetic interference, and a wide variety of light propagation patterns	Incapable of providing a continuous and real-time reaction

Table 2 Electrochemical sensing technology, physiological properties, and concentrations of associated sweat biomarkers

Bio-fluid	Biomarker	Concentration	Physiology or health condition	Sensing technique	Ref.
Sweat	Na <sup>+</sup>	10–100 mm	Dehydration, cystic fibrosis	Potentiometry	53
Sweat	Cl <sup>-</sup>	10–100 mm	Dehydration, cystic fibrosis	Potentiometry	53
Sweat	Lactate	5–20 mm	Anaerobic metabolism	Chronoamperometry	54
Sweat	Glucose	10–200 μM	Diabetes	Chronoamperometry	55
Sweat	Cortisol	8–140 ng mL <sup>-1</sup>	Blood pressure	EIS	56

a thorough understanding of the concentrations of each sweat species and their detecting principles.

### 2.1. Ions/pH electrochemical sensing principle

Sweat contains different types of ions at varying amounts (for instance, Na<sup>+</sup>, K<sup>+</sup>, Ca<sub>2</sub><sup>+</sup>, Cl<sup>-</sup>, NH<sub>4</sub><sup>+</sup>, H<sup>+</sup>, and OH<sup>-</sup> concentrations are all within the mm range). Potentiometry is the detection method for these ions. To measure Na<sup>+</sup>, K<sup>+</sup>, and pH using potentiometry, a solid contact ion-selective electrode comprised of a conductive substrate (electrode), a solid-contact, ion-selective membrane, and sweats forms the loop system that transforms the ion's activity to potential as the output signal. Ion-selective membranes are a hybrid material made of an ionophore, an ion exchanger, polymer matrix components, and plasticizers. They may respond selectively to certain ions.<sup>49</sup> Ionophore is the major element that exhibits a high selectivity for target ions.<sup>50</sup>

As auxiliary components, the ion exchanger, polymer matrix materials, and plasticizers all contribute to decreasing interference, maintaining mechanical support, and maintaining the membrane's homogeneity. To stabilize ion-to-electron transduction, a solid intermediary between the conductive substrate and the ion-selective membrane is required. The Nernst response equation is schematically depicted below. When the ionophore Nc in the ion-selective membrane comes into contact with sweat, it selectively absorbs target ions M<sup>+</sup> to generate MNc<sup>+</sup>. Nc<sup>+</sup> enters the membrane/solid contact interface following complexation and transfers electrons to the conductive substrate. There are two distinct processes for ion-to-electron transduction: redox reaction-based and double-layer

capacitance-based transducers.<sup>51</sup> The former is based on redox processes, whereas the latter forms an electrical double layer at the solid membrane/contact interface. When the ion content of the interfaces reaches a specific level, they create a potential difference. In an idealistic situation, potential fluctuations are only determined by the sweat/membrane interface due to the potential constants of other contacts. Based on the thermodynamic equilibrium principle and the Nernst equation, the activity of a target ion may be determined by measuring its potential value.<sup>52</sup>

$$\phi = \phi_0 + RT/zF \ln a$$

where  $\phi$  is the measured potential,  $\phi_0$  is the potential overall interfaces except the membrane/sweat interface.  $R$ ,  $T$ ,  $F$ ,  $z$ , gas constant, absolute temperature, Faraday constant, charge number of ion, and activity of the target sweat ion, respectively. From a sensing principle, the ion-selective membrane's exceptional selective recognition capacity and mechanical stability are critical, as they affect the level of sensitivity, selectivity, response time, and detection limit. On the other hand, long-term stability and repeatability are contingent on the solid transducer's features. An appropriate solid contact transducer must have a high redox capacity or a big capacitance to provide rapid ion-to-electron conversion.

### 2.2. Electrochemical sensing of biomolecules

The amperometric modality is used to detect the majority of sweat biomolecules. Cyclic voltammetry provides a programmable potential range that permits the electrode to oscillate between reduction and oxidation processes.





Chronoamperometry enables the determination of the change in current responsiveness with time for a desired electrochemical reaction. These two amperometric methods are extremely successful in measuring biomolecules such as sweat glucose, lactate, ethanol, uric acid, and ascorbic acid due to their rapid reaction and great sensitivity. Additionally, electrochemical impedance spectroscopy (EIS) is a highly effective technique for analyzing interface phenomena such as diffusion and the electric double layer. The information about the impedance of an electrochemical system may be obtained by applying an alternating current signal with modest amplitude and a varied frequency to it. EIS is a viable method for sweat cortisol detection because of the continual change in impedance throughout the electrode response.

### 3. Materials for sweat-ions detection

Over the years, tremendous efforts have been devoted to finding the optimal features of the membrane through regulating the components, and some practical membranes have been successfully adopted to detect the common cations in sweat ( $\text{Na}^+$ ,  $\text{K}^+$ , *etc.*). Examples of some of the materials used in the detection of analytes are as:

(a) Ion-Selective Membrane Electrode Materials for Detection of Sweat  $\text{Na}^+$ ,  $\text{K}^+$ ,  $\text{Ca}_2^+$ , and  $\text{NH}_4^+$ . Examples; 4-*tert*-butylcalix, arene-tetra acetic acid tetraethyl ester (Na ionophore X),<sup>57–59</sup> valinomycin,<sup>57,59,60</sup> *N*, *N*, *N'*, *N'*-tetracyclohexyl-3-oxapentanediamide (ETH-129),<sup>61,62</sup> and nonactin.<sup>63,64</sup>

(b) Polyaniline.<sup>65</sup>

(c) Silver Chloride for Detection of Sweat  $\text{Cl}^-$ .<sup>66</sup>

(d) Gold and Bismuth for Detection of Sweat  $\text{Zn}_2^+$ ,  $\text{Cd}_2^+$ ,  $\text{Pb}_2^+$ ,  $\text{Hg}_2^+$ , and  $\text{Cu}_2^+$ .

(e) Enzyme-Based Electrode Materials such as glucose oxidase (GOx), lactate oxidase (LOx), alcohol oxidase (AOx), uricase, urease, and ascorbate oxidase for the detection of sweat lactate, glucose, ethanol, and ascorbic acid.<sup>67</sup>

(f) Antibody-Based Electrode Materials for detecting Sweat Ethyl Glucuronide and Cortisol.

### 4. Wearable biochemical sensors for monitoring cystic fibrosis (CF)

The wearable sensor may identify sweat-related disorders by measuring molecular elements of sweat, such as chloride ions and glucose. A wristband wearable sweat sensor has the potential to evaluate cystic fibrosis, diabetes, and other illnesses diagnoses and medication assessment.<sup>68</sup> According to a study undertaken by experts at Stanford University School of Medicine in partnership with the University of California, Berkeley, the sensor gathers sweat, analyses its chemical composition, and then electronically communicates the data for analysis and diagnosis. Compared to traditional sweat collectors, the novel device does not need patients to remain immobile for an extended period while sweat accumulates in the collectors.<sup>68</sup>

Recently, wearable sweat sensors have received significant attention because of their importance in real-time monitoring

of various analytes in human sweat while engaging in physical activity. These sensors can provide exact sweat analyte measurements through signal processing and calibrations.<sup>69</sup> For instance, cystic fibrosis is a hereditary condition that damages the lungs and digestive system over time.<sup>69–71</sup> The carrier rate of cystic fibrosis in the US Caucasian population is approximately 5%. Sweat testing for the diagnosis of cystic fibrosis is currently conducted in two phases by highly trained, recognized laboratories. First, a suitable amount of sweat is collected and then transferred for chloride content measurement in a second step. Typically, the test requires two professionals and lasts a few hours. A sweat chloride level of  $\geq 60$  mM indicates a high risk of CF, but a sweat chloride level of  $< 30$  mM demonstrates that the condition is improbable.<sup>70</sup> Additionally, it is well established that the chloride-based sweat test and genetic analysis are insufficient for some CF patients with uncommon mutations. Still, the ratio of sweat sodium to chloride levels can assist in CF diagnosis.<sup>72</sup>

Emaminejada *et al.*<sup>73</sup> developed an electrochemically enhanced iontophoresis interface. It could easily extract sufficient sweat volume from patients without causing discomfort. Since it can be designed to create perspiration at pre-determined intervals, this interface can be utilized to acquire unprecedented insight into the secretion process. As a result, it can be used in personalized medicine to assess patients' responsiveness to modifying medications.

Based on the schematic representation in Fig. 2A, this platform comprises an electrode incorporating sweat induction and sensing electrodes that have been further combined with a wireless flexible printed circuit board (FPCB). The sweat can be directly analyzed on the secretion site by pasting the sensing electrode on the same substrate as the iontophoresis electrodes. The electrodes are printed on a mechanically flexible polyethylene terephthalate (PET) substrate to create a robust sensor skin contact. A small layer of agonist agent hydrogel sits between the sweat induction electrode and the skin. The sensing electrodes can be connected to the skin *via* a water-absorbent thin rayon pad. The hydrogels and sweat induction electrodes are also connected using thin stainless-steel connectors. Fig. 2B predicts potentiometric sodium and chloride sensors utilizing ion-selective films and an amperometric glucose sensor using glucose oxidase. The separate sensors and the iontophoresis process operate independently by electrically decoupling the switchable sweat sensing and sweat induction mode of operation. Blood glucose levels and iontophoresis-induced perspiration are connected, and sweat sodium and chloride levels are diagnostic markers for CF as depicted in Fig. 2C.<sup>73</sup> The target analyte is chosen for its usefulness in clinical diagnosis. The system-level overview of induction and sensing modes of operation is shown in Fig. 2D.

A safety mechanism is built into the sweat induction circuit to prevent skin from becoming overheated/or burning by employing a programmable current source and protection circuit with an upper limit for iontophoresis current. The device's circuits are constructed as a digitally programmable current source, ensuring that fluctuations in the skin conditions (such as conductivity and thickness) do not impact



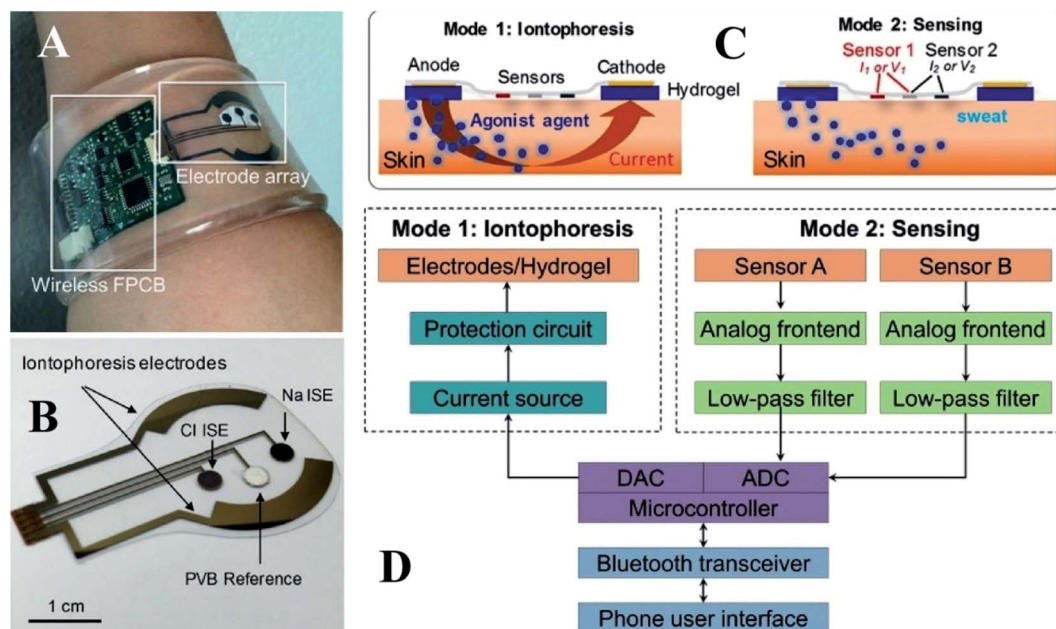


Fig. 2 (A) Self-contained sensing and sweat extraction platforms. (B)  $\text{Cl}^-$  and  $\text{Na}^+$  measuring iontophoresis and sweat sensor electrodes (C) schematic of sensing modes and iontophoresis (D) system-level block diagram of sensing circuits and iontophoresis<sup>73</sup> (Copyright 2017, National Academy of Science).

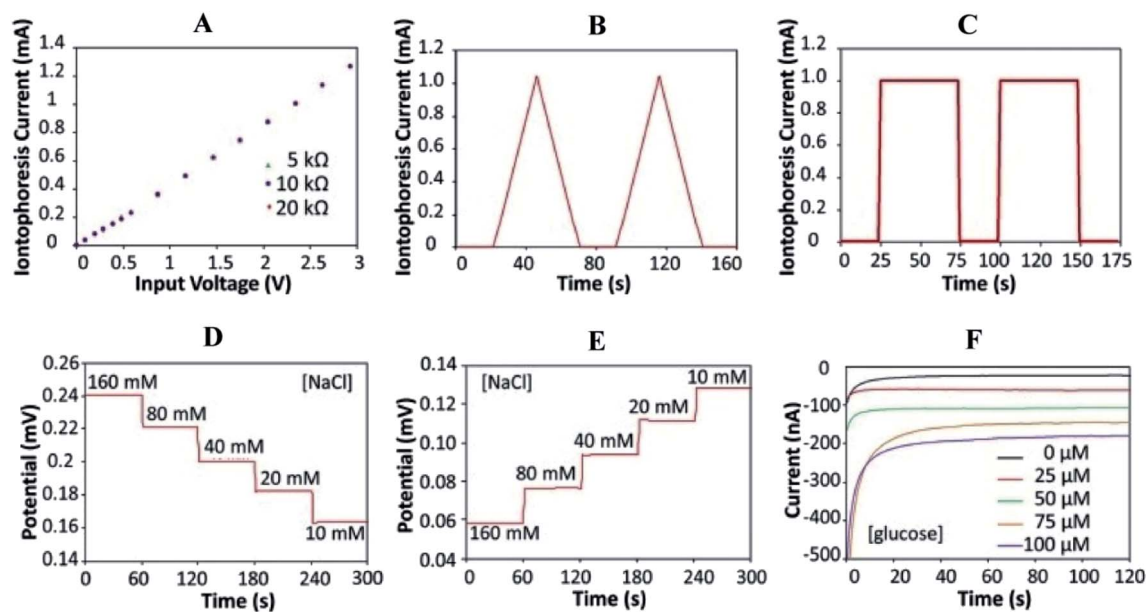


Fig. 3 Characterizations of the iontophoresis and sensing system. (A) Controlled iontophoresis current output for various resistive loads. (B and C) Programmed iontophoresis current to generate (B) saw tooth and (C) square wave patterns. (D and E) The open-circuit potential responses of the sodium (D) and chloride (E) sensors in NaCl solutions. (F) The chronoamperometric responses of a glucose sensor to glucose solutions. Data recording was paused for 30 s for each solution change.<sup>73</sup> (Copyright 2017, National Academy of Science).

iontophoresis performance. Fig. 3A depicts the circuit's programmability and current source behavior. Fig. 3B and C reveals the platform's capability to create iontophoresis current with saw tooth and square wave patterns. Fig. 3D and F shows the modified electrochemical sensors for sweat chloride, sodium, and glucose measurements. For chloride ion detection,

Ag/AgCl electrodes are utilized.<sup>74</sup> Whereas sodium ionophore X selectophore based ion-selective electrodes are used to measure sodium ions.<sup>53</sup> Polyvinyl butyral (PVB) coated electrodes containing saturated chloride ions are employed as reference electrodes because of their stable potentials in various analyte solutions.<sup>75</sup>



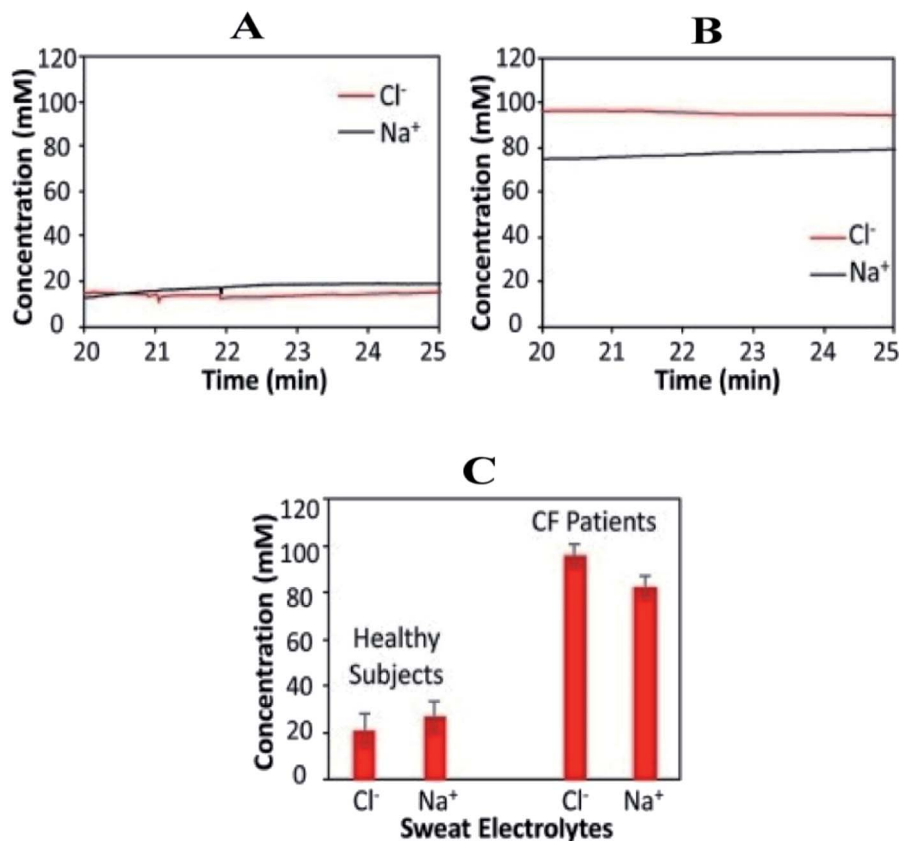


Fig. 4 Wearable sweat extraction and sensing system for CF diagnosis. (A) Real-time on-body measurement of a healthy subject's sweat sodium ion and chloride ion levels after iontophoresis-based sweat stimulation. (B) Real-time measurement of sweat sodium and chloride levels of a CF patient. (C) Comparison of sweat electrolyte levels between six healthy subjects and three CF patients.<sup>73</sup> (Copyright 2017, National Academy of Science).

Sweat testing is done in two steps by highly skilled recognized laboratories for CF diagnosis. Firstly, a significant amount of sweat is collected, and in the second step, it is transferred for chloride content determination. This examination requires the assistance of two professionals and takes a few hours to complete. If a sweat chloride level is  $> 60$  mM, it indicates a high chance of CF, whereas the disease is unlikely if it is  $< 30$  mM. This autonomous sensor is a reliable tool for early diagnosis and recovery of CF through on-demand sweat stimulations and simultaneous sodium and chloride sensing in sweat. It takes the form of a smart bracelet that patients can easily wear to induce excessive sweating. A 1 mA current is applied to the skin over 10 minutes, effectively delivering cholinergic agonists to the dermal space, where they can reach sweat glands. Sensors will detect a difference in potential between the working electrode and the reference electrode as soon as sweating begins.

According to the findings, the response is also stable around 20 minutes after iontophoresis, indicating an adequate amount of sweat production. The real-time body measurements of sweat electrolyte levels (20–25 min) for a healthy individual and a CF patient are shown in Fig. 4A and B, respectively. For CF patients, sweat chloride levels are higher than sweat sodium levels, whereas; sweat sodium levels are higher in healthy subjects

(Fig. 3C). The system is based on a microcontroller with accompanying analog circuitry for both iontophoresis current delivery and sensor reading. The microcontroller is connected to a bluetooth transceiver to interface the system to a cell phone. Finally, using the cell phone, the system could be commanded to transmit sensor readings in real-time or to output varying levels of iontophoresis current. The method proves to be effective—to establish a relationship between the physiological state of individuals and the sweat profile. It further facilitates the adoption of noninvasive sweat based sensing for diagnosis and screening of the general population. Ghaffari *et al.* recently investigated different sampling methods and analytical approaches for noninvasive clinical diagnostics for cystic fibrosis.<sup>88</sup>

## 5. Wearable biochemical sensors for lactate monitoring

Athletes' physical characteristics such as body temperature, heart rate, and workload are continuously measured throughout training and occasional tournaments. Chemical factors such as lactate, blood glucose, and electrolytes are examined by blood sample analysis before and after training. Thus, noninvasive, non-impeding approaches for monitoring



chemical parameters over time without interfering with training are desirable. As a result, various scientific investigations have been made to determine the chemical composition of released body fluids such as sweat, tears, saliva, and urine. In particular, sweat released by the Eccrine glands may be easily studied on the skin surface. Sweat includes electrolytes (such as sodium and potassium ions) and metabolites (such as lactate and glucose) at concentrations that coincide with those found in the blood.<sup>76,77</sup> Wearable sensors based on various detection techniques, such as electrochemical and colorimetric assays, have been produced in a variety of forms, including contact lenses, mouthpieces, and tattoo stickers.<sup>78,79</sup>

Lactate is a chemical biomarker that indicates anaerobic metabolism. The transformation of glucose to pyruvate does not require oxygen during glycolysis, the conversion of stored energy to useable energy, but the metabolism of the latter requires. When there is a concurrent oxygen deficiency and a demand for more energy, as occurs during exercise, pyruvate-lactate conversion provides useable energy. Still, it results in lactate buildup in the muscles, resulting in discomfort and exhaustion. Lactate is released into the circulation and sweated out of the body. As a result, lactate in sweat is viewed as a proxy for exercise [10].

Lactate monitoring *via* sweat is advantageous because it is easy to use, convenient, and correlates to blood lactate levels.<sup>80</sup> During intense workouts, hyperlactatemia patients and athletes must ensure proper oxygenation. Before exercising, lactate concentration in venous blood is 2.5–3.5 mM, and sweat lactate concentration is 13.7–27.1 mM.<sup>81</sup> As a result, the concentration of lactate in sweat is higher than blood before and after exercise. A rise in the amount of lactate excreted in sweat is an excellent indicator of metabolic acidosis, which can occur due to prolonged exercise.<sup>82</sup> Sweat lactate can be used for athletes to track their performance or exertion levels; hence, it can be used to measure the lactate threshold.<sup>24</sup>

A recent example of a sweat sensor detecting lactate was presented by Wenya *et al.* in 2019.<sup>83</sup> The author reported a wearable sweat analysis patch that could be easily mounted on human skin.<sup>18,83</sup> The silk NCT has six electrochemical sensors that detect biomarkers (lactate, AA, UA, Na<sup>+</sup>, K<sup>+</sup>, and glucose). The working electrode is a functionalized silk NCT that responds to hydrogen peroxide to detect lactate (Fig. 5).

However, this sensor patch was integrated with the signal collection and transmission circuit components to obtain real-time health monitoring of biomarkers in sweat. This smart sweat sensor patch was utilized to monitor the glucose content in a volunteer's sweat as a proof of concept. The findings were compared to those obtained using commercial high-performance liquid chromatography-mass spectrometry (HPLC-MS). This study establishes a potential technique for fabricating multiplex sweat analysis devices that are wearable.<sup>84</sup> Luke *et al.*<sup>85</sup> in 2018 demonstrated a wearable sensor system to monitor the concentration of lactate in sweat. Fig. 6A shows a silk NCT-based wearable multiplex sensor patch for *in situ* sweat analysis attached to human skin. Electrochemical sensors that allow simultaneous detection of six health-related indicators (glucose, lactate, AA, UA, Na<sup>+</sup>, and K<sup>+</sup>) as depicted in Fig. 5B. Silk NCT was employed as the working electrodes of the flexible electrochemical sensors either alone or in combination with other substances. The circuit was created from a conductive Ni-coated cloth tape using a facile digital laser writing technique. The flexible patch, shown in Fig. 6C, can be conformably applied to the human body for *in situ* sweat analysis. Wearable sweat sensor patches manifest consistent results with glucose concentration in the volunteer's sweat—which is an indication of good potential and reliability of the wearable sweat analysis patch for non-invasive health monitoring.

The electronic patch is coated with an adhesive for allowing it to be easily removed and replaced if the sensor's performance is compromised. It can be used as a smart adhesive bandage in

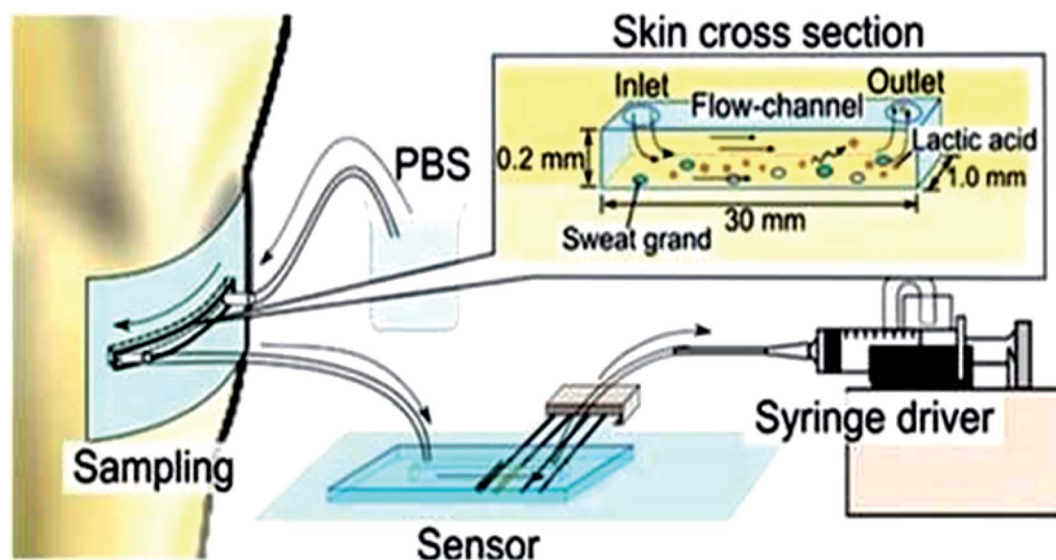


Fig. 5 Lactic acid monitoring system showing schematic representation.<sup>86</sup> (Wiley Periodicals, Inc).





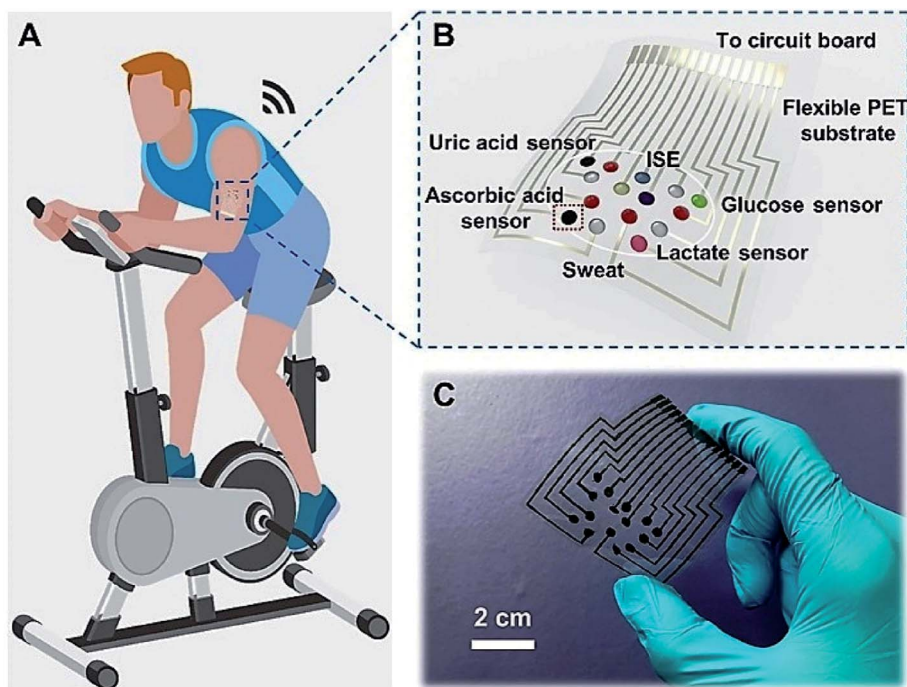


Fig. 6 Silk NCT based wearable sweat analysis patch (A and B). Graphical illustration of human skin mounts for sweat analysis patch and integration of multiplex electrochemical sensor array in the patch (C) photographic representation of wearable sweat patch analysis.<sup>83</sup> (Photo credit: Wenya He, Tsinghua University Wenya He *et al.* *Sci Adv* 2019).

various situations. An organic electrochemical transistor (OECT) was integrated into a stand-alone system to develop this sensor first. For the gate electrode, which catalyses the reduction of hydrogen peroxide, either platinum or Prussian blue coated with lactate oxidase (LOX) was used, depending on the application. The gate electrode makes donations of electrodes that raise the gate potential by a factor of two. As a result, de doping of the channel occurs when the gate voltage is positive. As the gate potential is raised, the channel conductivity decreases, which results in the magnitude of the drain current

reducing and increasing the gate potential. As a result, the drain current would decrease as the concentration of lactate increased in the blood. The lactate sensing ability of this sensor is limited to a concentration of less than 1 mM of LOX in the environment. They reported non-linear responses as well as high sensitivity to the stimuli. The advantage of this electronic patch is that its sensing element can be easily replaced and removed if it ages in a way that affects performance.

The same year, Keigo *et al.*<sup>86</sup> developed a microfluidic system for lactic acid monitoring at the skin's surface (Fig. 7). It

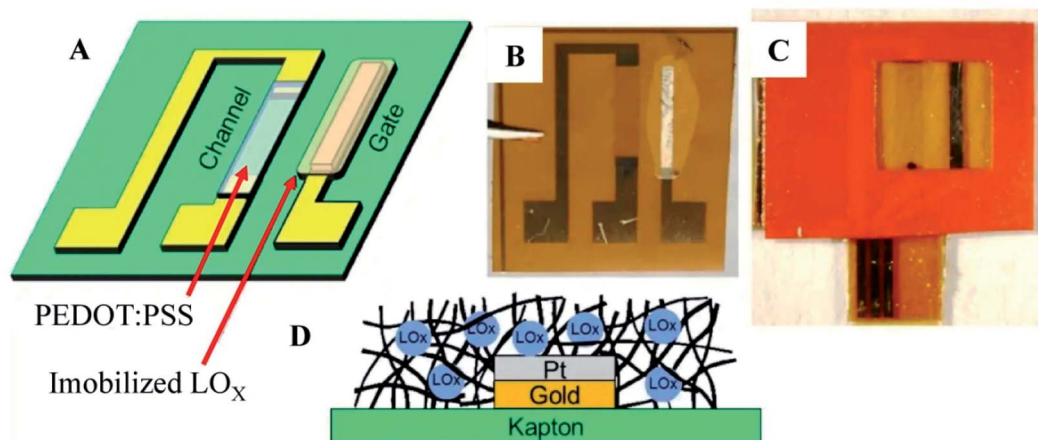


Fig. 7 Lactate sensing in sweat by Organic Electrochemical Transistor. (A) Conceptual drawing of device. (B) Photograph depicting immobilized lactate oxidase (LOx) plate gate functionalization device (C) Vinyl sticker applied for confining solution above the channel region of OECT and active gate (D) Immobilization of LOx in notional glutaraldehyde matrix.<sup>85</sup> (Nature Publishing Group).



measures changes in lactate secretion as a function of exercise intensity. This sensor comprises polydimethylsiloxane (PDMS) attached to the skin surface and connects to sweat glands. PBS is used as a carrier fluid to dissolve the entire secretion, and the discharged LA is measured. This study demonstrates that the rate of change of lactate secretion and perspiration are significantly different and vary independently, reflecting the quality of the exercise. It has been deemed beneficial for sports training and highlights changes in an individual's physiological state. This flow type measurement device results exhibited a big difference in change rate between lactate secretion and perspiration. They both change independently with exercise intensity.

There are a few other noteworthy works in this field. Sweat sensors are made of PVC polymer, but they use it as a membrane to increase the sensor's sensitivity. When a diffusion limiting PVC membrane is implemented in a LOX based working electrode (for instance TTF mediated); Zamarayeva *et al.* discussed how it affects sensor performance and how these membranes are essential for a wearable sweat sensor to perform continuous lactate measurements because the internal diffusion of the membrane is remarkably lower than the external diffusions.<sup>87</sup> Also, Nagamine *et al.* demonstrated a touchpad covered with an agarose gel in a phosphate buffer saline solution for lactate measurements.<sup>88</sup> Hong *et al.* developed a device composed of a strip integrating both a glucose and lactate sensor that can provide the physiological data, glucose and lactate levels pre-or-post exercise.

For lactate and other electrolytes monitoring, Mohan *et al.*<sup>89</sup> described the challenges and feasible solutions. However, the major challenge remains with the feasibility of electrode materials with appropriate mechanical properties. The typical electrochemical sensors depend on bulky electronic devices, which are rigid and heavy. This makes them incompatible with wearable applications. To facilitate conformal integration with the epidermis and to sustain repeated multi-axial mechanical distortions; the transformation of hard planar systems into flexible, soft and miniature devices is greatly required.

## 6. Wearable biochemical sensors for monitoring diabetes

The primary source of energy in a living body is glucose. Maintaining proper glucose concentration in the blood and the homeostatic system is essential.<sup>90</sup> According to the World Health Organization (WHO); roughly 5% of the global population has diabetes.<sup>90</sup> Hyperglycemia could lead to other life-threatening diseases including heart attack, heart failure, and adult blindness.<sup>91</sup> While, hypoglycemia can lead to coma/or death. Therefore, it is mandatory for diabetic patients to regularly monitor blood glucose levels. It can be done *via* blood glucometers or continuous glucose monitoring devices. Former is invasive and painful; resulting in the need to develop the latter device, which is non-invasive and painless. Recently, Benoit *et al.*<sup>92</sup> reviewed the significant applications of sweat analysis in wearable non-invasive sensors.

Moyer *et al.* in 2012, focused on the rapid sweat sampling without contamination from the skin, and examined a strong correlation between blood and sweat glucose concentrations in diabetes patients.<sup>93</sup> To generate sweat, iontophoretic stimulations by pilocarpine drug delivery have been used. While the perfusion method has been used to collect the generated sweat. Soap, water, and 70% isopropanol have removed glucose residue from the skin surface. Such investigations revealed the necessity for effective sweat collection systems free of contamination from the skin's surface and sensitive detection platforms that can be calibrated continuously.

Furthermore, Gao *et al.* described a flexible and integrated sensor array platform to measure multiple sweat metabolites in a wearable patch type platform.<sup>69</sup> For practical realization of this wearable sensor, it was integrated signal transduction, processed and wireless transmitted. This device was worn on the forehead, wrist, or arms (Fig. 8).

The varying sweat flow rates are seen during real-time sweat monitoring during exercise. GOX and Prussian blue catalyzed reactions lead to amperometric glucose detection. The measured sweat glucose concentration decreases with continuous exercise. Elevation in skin temperature was observed with an increase in sweat rate and dilution of sweat glucose over time. The high-temperature impacts the enzyme (GOX) activity, which must be considered to avoid overestimating actual glucose concentration. The study further claims that careful sweat rate, environmental parameters, and sweat composition are required for accurate blood glucose level monitoring. The entire system is mechanically flexible, so the wearable sensor technology can be used for prolonged outdoor and indoor physical activities. The system could be exploited/or reconfigured for *in situ* analyses of other biomarkers within other human fluid samples and sweat to facilitate personalized and real-time physiological and clinical investigations. Hyunjae lee *et al.* in 2017 discussed a device for sweat glucose monitoring integrated with a transdermal drug delivery module. The patch is reusable and works under different temperatures effectively. It starts monitoring with humidity sensing, then the sweat glucose and pH levels are detected by glucose and pH sensors, respectively. Once the sweat uptake layer absorbs a significant amount of sweat, the disposable strip type sensor starts monitoring by absorbing sweat first. It is then connected to hardware *via* a ZIF connector for sweat analysis.

As confirmed by statistical analysis, blood glucose levels measured *via* commercial glucose meter correlate with the sweat glucose levels measured by disposable and wearable sweat glucose sensors Fig. 9. For practical application of the system to human subjects with minimum recalibrations, the long-term stability and uniformity of sensors are particularly very important. But further studies about the correlation between glucose levels of sweat and blood are needed before application to diabetic patients. Furthermore, metformin is used in the system and due to its working mechanism; it shows suppression of the blood glucose levels. Although with further improvements in these points, clinical translation can be pursued for feedback therapy and sweat based sensing. It also provides important new advances towards the stress-free point-



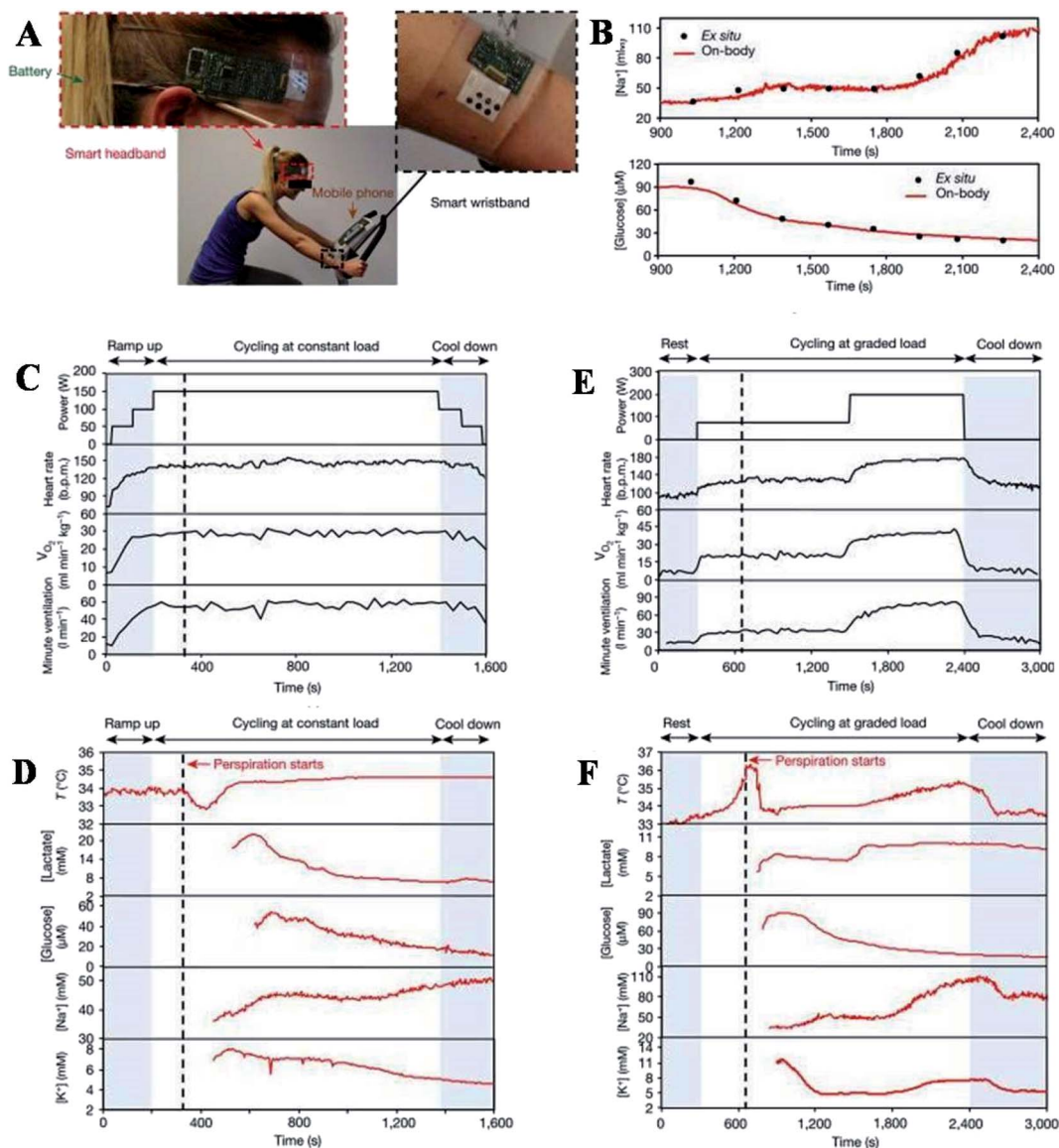


**Fig. 8** On-body real-time perspiration analysis during stationary cycling: photographs of a subject wearing (A) 'smart headband' and a 'smart wristband' during stationary cycling. (B) Comparison of *ex situ* calibration data of the sodium and glucose sensors from the collected sweat samples with the on-body readings of the FISA during the stationary cycling exercise detailed in (F). (C and D) Constant-load exercise at 150 W: power output, heart rate (in beats per minute, bpm), oxygen consumption ( $V_{O_2}$ ) and pulmonary minute ventilation, as measured by external monitoring systems (C) and the real-time sweat analysis results of the FISA worn on a subject's forehead (D). (E and F) Graded-load exercise, involving a dramatic power increase from 75 W to 200 W: power output, heart rate,  $V_{O_2}$  and pulmonary minute ventilation, as measured by external monitoring systems (E) and the real-time analysis results using the FISA worn on a different subject's forehead (F) nature.<sup>69</sup>

of-care and painless treatment of diabetes mellitus. Karpova *et al.* discussed another approach using flow outlets to monitor glucose.<sup>94</sup> It stated that undiluted sweat right after its excretion could be continuously analyzed using the flow-through glucose biosensor. They used glucose oxidase dipped in isopropanol onto the surface of Prussian blue and immobilized in perfluoro sulfonic ionomer or siloxane gel. Based on the glucose tolerance test, the Pearson correlation coefficient was 0.75, meaning that glucose concentration variation rates in blood and sweat correlate positively.<sup>94</sup> Diabetic patients can monitor blood content *via* continuous analysis of the excreted sweat, significantly decreasing blood probing. Considerable efforts have

been made for the development of noninvasive real-time glucose-sensing techniques.<sup>95–98</sup> However, further efforts can improve the quality of life for hundreds of millions of people in this direction.

## 7 BP and biomarker monitoring

Blood pressure is the force that blood exerts on the walls of blood-carrying microtubes (*i.e.*, arteries and veins) due to the heart's periodic contraction and relaxation. Special nerve receptors called baroreceptors located in the arterial wall detect blood pressure.<sup>99</sup> Mechanoreceptors in the skin are critical for sensing touch, tickling, and other bodily interactions.





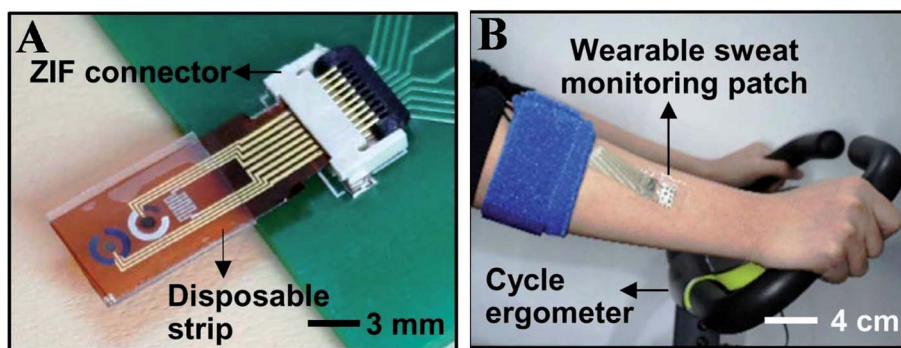


Fig. 9 (A) Optical camera image of the disposable strip-type sensors connected to a zero insertion force (ZIF) connector. (B) Optical camera image of the subject using a cycle ergometer for sweat generation with the wearable patch on the subject's arm (Science advances).<sup>123</sup>

Additionally, they contribute significantly to detecting mechanical stimuli such as pressure, torsion, friction, bending, vibration, and stretching.<sup>99</sup> Proprioceptors are another type of receptor that is crucial for feeling the body's position, force, and other motions. They are also necessary for spatial perception, which enables precise control of bodily interactions with the environment, such as walking, gripping things, and recognizing textures.<sup>99,100</sup>

Pressure sensors are equally crucial elements in e-skin for pressure sensing in the human body. These pressure sensors aim to discriminate normal and shear forces, tensile strength and vibrations in the context of robotics and prosthetics—for the sense of grabbing items and manipulation, feeling textures, or replicating proprioception.<sup>100</sup> Wearable sensors are used to achieve specific values for monitoring various health problems. Pressure sensors can be used to monitor blood pressure wave (BPW), heart rate, body motions, breathing, and others.<sup>2,100,101</sup>

Flexible pressure sensors were used to capture the dynamic biomarkers and blood pressure fluctuations during physical activity. In this study, physically active people are likely to have a lower resting blood pressure, considerably lowering the risk of heart failure by a significant amount.<sup>102,103</sup> During exercise, the resting blood pressure can be reflected in a smaller increase, like the physically active people signal the body to produce nitric oxide earlier to promote increased vasodilation.<sup>102</sup> Physically active people are also predicted to have lower lactate concentration levels than non-active people.<sup>2</sup> Regardless of fitness level, an individual's blood pressure should decline after strenuous exercise activity and finally return to its original value.<sup>104</sup> Furthermore, a research study has found a link between the extent of the post-exercise falls in blood pressure and lactate levels, demonstrating that higher blood lactate levels following a high-intensity exercise promotes high differences between pre-and post-exercise blood pressure values.<sup>105</sup> Thus, to study such complex dynamic processes in-depth, hybrid wearable sensors need to continuously capture and analyze these real-time fluctuations throughout the activity. One more research study has been conducted in which individuals with varying levels of fitness (physically active and inactive) were asked to cycle for 30 minutes at a constant intensity while wearing the device (during the entire experiment), and their blood pressure and lactate levels were

monitored continuously until the exercise was stopped. Sweat was produced naturally as a result of the physical activity, and in this study, iontophoresis (IP) was not used in this section. Before, 10 minutes into, and after the workout, validation data were collected. The sedentary individuals had significantly higher sweat-lactate levels and elevated blood pressure values than the active individuals during the activity (as indicated in Fig. 10a and b).

During exercise, physically inactive people are likely to have heart rate (HR), blood pressure (BP), and sweat-lactate levels due to higher catecholamine concentration than physically active people, resulting in blood pressure differences based on fitness levels cardiovascular system.<sup>106</sup> One more research study to predict blood pressure using flexible polymer transistors with high-pressure sensitivity for electronic skin and health monitoring application. In this study, the sensitivity of flexible polymer transistors with sensitivity (8.4 kPa) in a low-pressure regime was found to be  $< 8$  kPa. When related to the recent reports on flexible pressure sensors, combination with its fast response time ( $< 10$  ms) is extraordinary. Further, the outcome of this investigation demonstrated high sensitivity in activating the thin-film transistor in the sub-threshold zone. The sub-threshold operation in Si nanowire biosensors and organic thin-film transistors (OTFTs) temperature sensors has been proposed to lower integrated power circuit consumption and boost sensitivity.<sup>107,108</sup>

Another research study discovered that piezoelectric sensors have high dynamic pressure sensitivity, but sensing actual static pressure requires complex support electronics.<sup>109</sup> Pang *et al.* studied that pressure sensors based on interlocked arrays of Pt-coated polymeric nanofibers with great sensitivity but the incorrect response to pressure changes to  $> 1$  Hz.<sup>110</sup> Further, microstructured polydimethylsiloxane (PDMS) was recently reported as a dielectric layer for flexible capacitive pressure sensors with  $0.55 \text{ kPa}^{-1}$  sensitivity and millisecond response time.<sup>111</sup> The use of a microstructured PDMS dielectric in conjunction with a thin-film polymer semiconductor in this exercise allowed us to create a flexible plastic pressure-sensitive device that significantly improved sensitivity outcomes even at extremely low pressure because the transistor is in a sub-threshold state but still has a lightning-quick response time.





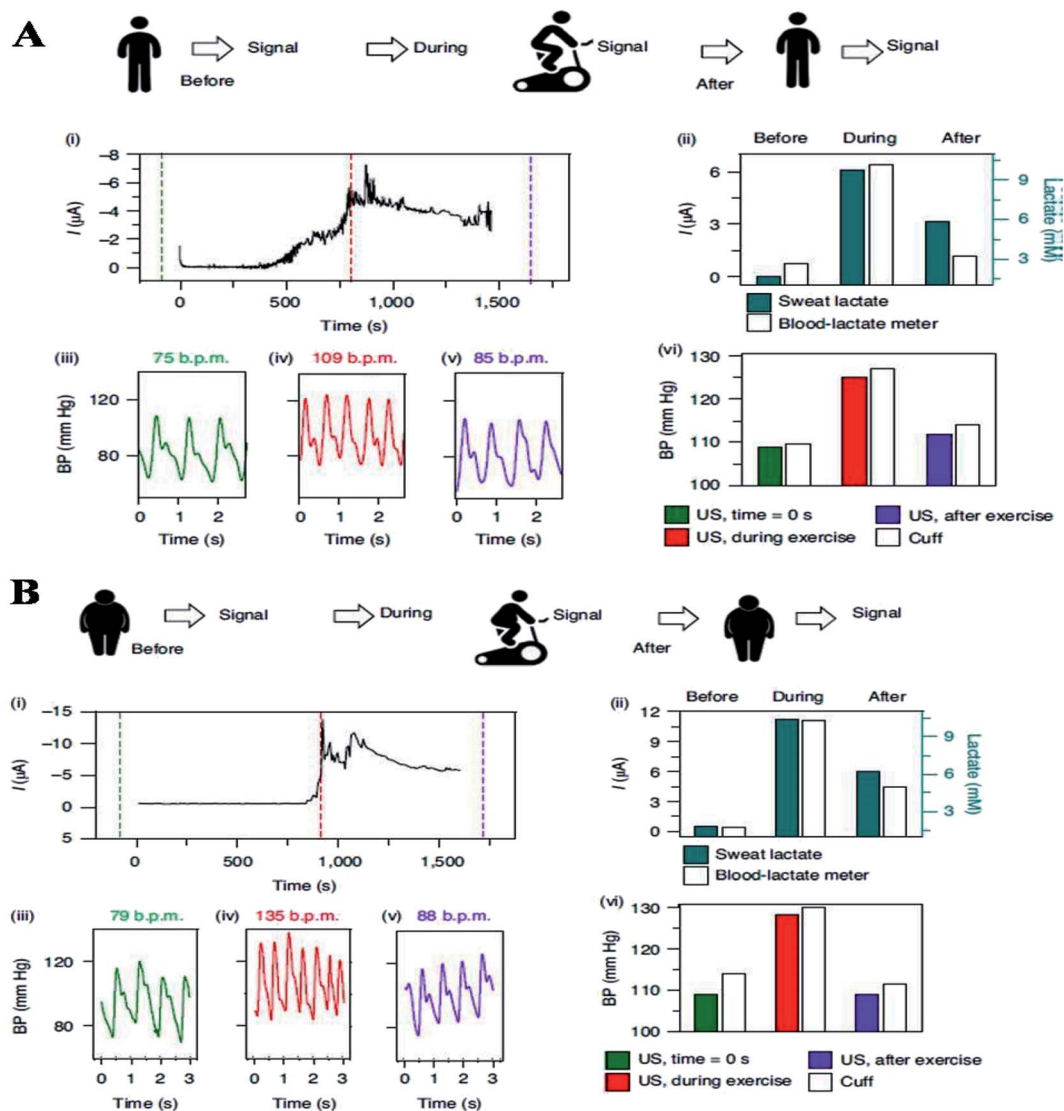


**Fig. 10** (A) Experiments showing the current body assessment for measuring heart rate, blood pressure, and continuous lactate in an active volunteer (top). (i) the Sweat-lactate profile was assessed by continuous signal recording during stationary cycling sweat-lactate profile. The dashed lines show time corresponding to the plotted BP data before, during, and after exercise. (ii) The data was validated using electrochemical sensor readings and commercial blood lactate metres (iii)–(v) heart rate and blood pressure recording before (iii), during (iv), and after (v) stationary cycling. (vi) The comparative assessment of blood pressure signals obtained with ultrasound (US) transducers and commercial cuff before, during, and after the exercise. (B) Continuous current recording during stationary cycling, displaying the sweat-lactate profile. Dashed lines mark the time corresponding to the plotted BP data (before, during and after exercise) (before, during and after exercise). (ii) Validation with a commercial blood lactate meter and electrochemical sensor readings (iii) and (iv), heart rate and blood pressure recording (iii), during (iv), and after (v) stationary cycling. (vi) Before, during, and after the exercise activity, a comparison of the BP signal from a commercial cuff and the US transducers.<sup>124</sup>

Sheng li *et al.* concluded the different materials selection and fabrication for the wearable microfluidic sensors for glucose, lactate and other electrolytes sensing.<sup>90</sup> The paper-based microfluidic platforms have not achieved the wearable goals and great efforts have recently been made for the selection of suitable substrate materials for fabricating wearable microfluidic sensors. The selection of suitable substrates will improve the sensing performance and wearability of microfluidic sensors which further extends its applications. The substrate materials, including fabrics and polymers are widely used due to their excellent biocompatibility, inherent flexibility and

stretchability. The microfluidic sensors can be classified according to the substrate materials *i.e.*, fabric-based microfluidic platforms and polymer-based microfluidic platforms. The fabric-based microfluidic sensors need simple textile processing methods and it has great potential for large-scale manufacture.<sup>91</sup> The polymer-based microfluidic platforms possess attractive physical features such as biocompatibility, optical transparency, excellent flexibility, stretchability and low modulus.<sup>92,93</sup> Therefore, it is widely used in wearable sensors. Basically, polymeric microfluidic substrates are mainly based on elastomer—including ecoflex, poly(dimethylsiloxane)



(PDMS), and poly(styreneisoprene) (SIS) (94–96). Among these three materials, PDMS is the most widely used in microfluidic sensors due to its mature and low cost and simple manufacturing methods. The most common technique for the fabrication of elastomer-based microfluidic networks is soft lithography based on patterned silicon molds. These sensors have wide application for diagnosing BP, diabetes and lactate concentrations.

## 8. Wearable biochemical sensors for tuberculosis monitoring

Tuberculosis (TB) cure needs patients to adhere to a multidrug regimen for a minimum of six months.<sup>112,113</sup> Inappropriate administration of medicines—results in concern public health (including drug resistance, treatment failure, and tuberculosis transmission). These implications were illustrated in New York City (in the late 1980s), when almost half of the patients initiated on medication failed to finish it. And, the incidence of drug-susceptible and multidrug-resistant tuberculosis (MDR) TB spiked.<sup>114</sup> Similar events in Africa have recently risen to extensively drug-resistant tuberculosis (XDR) TB, a practically incurable form of the illness.<sup>115</sup> The public health consequences of non-adherence to active TB treatment led to directly observed therapy (DOT) becoming the standard of care in the US. and around the world.<sup>112,116–118</sup>

Despite the availability of therapy, vaccines, and other control efforts to combat tuberculosis, it remains a severe concern to the global community.<sup>119</sup> The typical symptom of TB is excessive sweating. However, the use of sweat diagnoses is still largely unexplored.<sup>120</sup> To our knowledge, Adewole *et al.*<sup>121</sup> have conducted the first proteomic study on sweat from TB patients. To look for potential biomarkers of active TB, they examined proteomics between active TB, non-TB, and healthy people. It is a viable approach to develop a non-sputum-based test for the detection of active TB. They detected twenty-six disease-specific proteins. These results need further verification and studies for individual patient samples for robust statistical analysis. It can also be used to determine the effectiveness of antibiotic chemotherapy by monitoring changes in the sweat of patients undergoing the treatment course.

## 9. Conclusion and future perspectives

Wearable sweat sensors have generated considerable interest due to their noninvasive operation style, real-time availability, and several application possibilities in the healthcare industry. Over the last decade, significant attention has been paid to the development of wearable sweat sensors capable of collecting, detecting, and displaying sweat data. Two of these prerequisites for exploiting human perspiration are sweat secretion and collecting. Iontophoresis, which involves injecting an agonist directly into sweat glands, is a promising approach for inducing *in situ* sweating. On the other hand, iontophoresis continues to have concerns with delayed measurement and current

stimulation, leading to errors in the results. Sweat collection is complex under normal conditions due to the low volume of secretion, rapid volatilization, and varied levels of secretion in various parts of the body.<sup>122</sup> Microfluidic-based methods have made major advances in this area. Thus, several microfluidic sweat systems have been crafted.

The human “body-on-chip” technologies mimic organ–organ interactions, which are critically helpful for disease modeling, and discovering new and precise medicines. Nonetheless, it is still impossible to recapitulate some clinical manifestations examined using animal models, such as vomiting or diarrhea. Compared to the *in vitro* systems, “body-on-chip” systems provide better *in vivo* mimicry models at the cell, tissue, and organ levels. They are often more predictive of human outcomes than *in vivo* models in many cases. The present short review discusses the sweat sensors with applications in health care (monitoring the chronically ill patients) and athletic training (monitoring body fitness). Recently, sweat biomarkers have been researched thoroughly investigated for real-time diagnoses of diseases non-invasively. Due to the rapid flow in miniature microfluidic channels; sweat sensors improve both sensitivity and efficiency—while reducing sweat concentration. Various sensing principles, including colorimetric, fluorometric, and electrochemical, have been used in microfluidic-based sensors. The rapid advancement of microfluidic devices in industry and healthcare has made it possible to combine various sensors into a single miniature wireless multiplex device to detect multiple biomarkers in sweat. Nonetheless, continuous research is needed to make sensors self-powered and wireless.

Lately, extensive efforts have been made to diagnose cystic fibrosis by monitoring sweat analytes using signal processing and calibrations. Similarly, several sensing technologies have been developed for the real-time monitoring of lactate and glucose. Any variation of glucose concentration in blood and sweat was found to be positively correlated. It is vital to look at the relationship between biomarker concentrations in blood and sweat. Furthermore, non-sputum-based tests can also be explored to detect TB.

Noticeably, the field is unknown and demands comprehensive research and development. However, “body-on-chip” technology is still nascent, and various obstacles must be solved before it gains physiological relevance and is translated into the clinic. The advancement could include new cell subtypes, organ-specific microbiomes and metabolites, and biochemical and biophysical gradients across the linked organs to chip models. Scaling up the “body-on-chip” systems allometrically, metabolically is highly recommended. In addition, depending upon the actual organ sizes *in vivo* to simulate physiological reactions and to adjust the fluid volume and dynamics in chips according to individual human organs, all of which are crucial to mimic physiological responses. Liquid-to-cell (volume) ratios should be co-related to reflect the physiological well-being of humans. Addressing these challenges would outline the way forward for personalized “body-on-chip” devices for tailored diagnosis and seamless disease monitoring. We believe “body-on-chip” technology will revolutionize the healthcare system on



various fronts in developed and emerging nations. It will significantly reduce the healthcare system's cost, improve life expectancy by fifteen to twenty years, and reduce animal usage for clinical trials.

## Conflicts of interest

There is no conflict of interest.

## Acknowledgements

This work is supported by SERB (Science & Technology Research Board), a statutory body under the Department of Science & Technology, Government of India; under the Research grant of Ramanujan Fellow Award (File number: SB/S2/RJN-013/2018).

## References

- 1 L. Meng, A. P. F. Turner and W. C. Mak, *Biotechnol. Adv.*, 2020, **39**, 107398.
- 2 Y. Yamamoto, S. Harada, D. Yamamoto, W. Honda, T. Arie, S. Akita and K. Takei, *Sci. Adv.*, 2016, **2**, e1601473.
- 3 M. Amjadi, K. U. Kyung, I. Park and M. Sitti, *Adv. Funct. Mater.*, 2016, **26**, 1678–1698.
- 4 T. Q. Trung and N. E. Lee, *Adv. Mater.*, 2016, **28**, 4338–4372.
- 5 J. Cao, C. Lu, J. Zhuang, M. Liu, X. Zhang, Y. Yu and Q. Tao, *Angew. Chem.*, 2017, **129**, 8921–8926.
- 6 X. Liu, C. Lu, X. Wu and X. Zhang, *J. Mater. Chem.*, 2017, **5**, 9824–9832.
- 7 C. Luo, J. Jia, Y. Gong, Z. Wang, Q. Fu and C. Pan, *ACS Appl. Mater. Interfaces*, 2017, **9**, 19955–19962.
- 8 S. Bauer, S. Bauer-Gogonea, I. Graz, M. Kaltenbrunner, C. Keplinger and R. Schwödiauer, *Adv. Mater.*, 2014, **26**, 149–162.
- 9 S. Ye, S. Feng, L. Huang and S. Bian, *Biosensors*, 2020, **10**, 205.
- 10 M. Dervisevic, M. Alba, B. Prieto-Simon and N. H. Voelcker, *Nano Today*, 2020, **30**, 100828.
- 11 N. Brasier and J. Eckstein, *Digit. Biomark.*, 2019, **3**, 155–165.
- 12 J. Kim, S. Imani, W. R. de Araujo, J. Warchall, G. Valdés-Ramírez, T. R. L. C. Paixão, P. P. Mercier and J. Wang, *Biosens. Bioelectron.*, 2015, **74**, 1061–1068.
- 13 J. Choi, A. J. Bandodkar, J. T. Reeder, T. R. Ray, A. Turnquist, S. B. Kim, N. Nyberg, A. Hourlier-Fargette, J. B. Model and A. J. Aranyosi, *ACS Sens.*, 2019, **4**, 379–388.
- 14 K. Mahato and J. Wang, *Sens. Actuators, B*, 2021, 130178.
- 15 S. Jo, D. Sung, S. Kim and J. Koo, *Biomed. Eng. Lett.*, 2021, 1–13.
- 16 S. A. Iyengar, P. Srikrishnarka, S. K. Jana, M. R. Islam, T. Ahuja, J. S. Mohanty and T. Pradeep, *ACS Appl. Electron. Mater.*, 2019, **1**, 951–960.
- 17 R. K. Mishra, L. J. Hubble, A. Martín, R. Kumar, A. Barfidokht, J. Kim, M. M. Musameh, I. L. Kyratzis and J. Wang, *ACS Sens.*, 2017, **2**, 553–561.
- 18 H. Teymourian, A. Barfidokht and J. Wang, *Chem. Soc. Rev.*, 2020, **49**, 7671–7709.
- 19 J. Kim, A. S. Campbell, B. E.-F. de Ávila and J. Wang, *Nat. Biotechnol.*, 2019, **37**, 389–406.
- 20 A. J. Bandodkar and J. Wang, *Trends Biotechnol.*, 2014, **32**, 363–371.
- 21 Y. Yang and W. Gao, *Chem. Soc. Rev.*, 2019, **48**, 1465–1491.
- 22 D. Rodrigues, A. I. Barbosa, R. Rebelo, I. K. Kwon, R. L. Reis and V. M. Correlo, *Biosensors*, 2020, **10**, 79.
- 23 K. D. Long, E. V. Woodburn, H. M. Le, U. K. Shah, S. S. Lumetta and B. T. Cunningham, *Lab Chip*, 2017, **17**, 3246–3257.
- 24 S. Imani, A. J. Bandodkar, A. M. V. Mohan, R. Kumar, S. Yu, J. Wang and P. P. Mercier, *Nat. Commun.*, 2016, **7**, 1–7.
- 25 H. Zhu, D. Liu, D. Zou and J. Zhang, *J. Mater. Chem.*, 2018, **6**, 6130–6154.
- 26 X. Zhu, S. Yuan, Y. Ju, J. Yang, C. Zhao and H. Liu, *Anal. Chem.*, 2019, **91**, 10764–10771.
- 27 G. Li and D. Wen, *J. Mater. Chem. B*, 2020, **8**, 3423–3436.
- 28 E. Matysiak-Brynda, J. P. Sęk, A. Kasprzak, A. Królikowska, M. Donten, M. Patrzalek, M. Poplawska and A. M. Nowicka, *Biosens. Bioelectron.*, 2019, **128**, 23–31.
- 29 C. Lucarotti, C. M. Oddo, N. Vitiello and M. C. Carrozza, *Sensors*, 2013, **13**, 1435–1466.
- 30 R. S. Dahiya, P. Mittendorfer, M. Valle, G. Cheng and V. J. Lumelsky, *IEEE Sens. J.*, 2013, **13**, 4121–4138.
- 31 C. Hou, H. Wang, Q. Zhang, Y. Li and M. Zhu, *Adv. Mater.*, 2014, **26**, 5018–5024.
- 32 H. Li, C. X. Luo, H. Ji, Q. Ouyang and Y. Chen, *Microelectron. Eng.*, 2010, **87**, 1266–1269.
- 33 R. D. P. Wong, J. D. Posner and V. J. Santos, *Sens. Actuators, A*, 2012, **179**, 62–69.
- 34 C.-Y. Wu, W.-H. Liao and Y.-C. Tung, *Lab Chip*, 2011, **11**, 1740–1746.
- 35 Y.-L. Park, C. Majidi, R. Kramer, P. Bérard and R. J. Wood, *J. Micromech. Microeng.*, 2010, **20**, 125029.
- 36 A. Koh, D. Kang, Y. Xue, S. Lee, R. M. Pielak, J. Kim, T. Hwang, S. Min, A. Banks and P. Bastien, *Sci. Transl. Med.*, 2016, **8**, 366ra165.
- 37 Y. S. Rim, S.-H. Bae, H. Chen, J. L. Yang, J. Kim, A. M. Andrews, P. S. Weiss, Y. Yang and H.-R. Tseng, *ACS Nano*, 2015, **9**, 12174–12181.
- 38 H. Lee, T. K. Choi, Y. B. Lee, H. R. Cho, R. Ghaffari, L. Wang, H. J. Choi, T. D. Chung, N. Lu and T. Hyeon, *Nat. Nanotechnol.*, 2016, **11**, 566–572.
- 39 K. O. Kim, G. J. Kim and J. H. Kim, *RSC Adv.*, 2019, **9**, 22790–22794.
- 40 J. Choi, R. Ghaffari, L. B. Baker and J. A. Rogers, *Sci. Adv.*, 2018, **4**, eaar3921.
- 41 M. Chung, G. Fortunato and N. Radacsi, *J. R. Soc., Interface*, 2019, **16**, 20190217.
- 42 J. Heikenfeld, A. Jajack, J. Rogers, P. Gutruf, L. Tian, T. Pan, R. Li, M. Khine, J. Kim and J. Wang, *Lab Chip*, 2018, **18**, 217–248.
- 43 J. Kim, I. Jeerapan, J. R. Sempionatto, A. Barfidokht, R. K. Mishra, A. S. Campbell, L. J. Hubble and J. Wang, *Acc. Chem. Res.*, 2018, **51**, 2820–2828.
- 44 M. Mayer and A. J. Baeumner, *Chem. Rev.*, 2019, **119**, 7996–8027.



- 45 Q. Zhai and W. Cheng, *Mater. Today Nano*, 2019, **7**, 100041.
- 46 A. Nemiroski, D. C. Christodouleas, J. W. Hennek, A. A. Kumar, E. J. Maxwell, M. T. Fernández-Abedul and G. M. Whitesides, *Proc. Natl. Acad. Sci.*, 2014, **111**, 11984–11989.
- 47 Y. Yu, H. Y. Y. Nyein, W. Gao and A. Javey, *Adv. Mater.*, 2020, **32**, 1902083.
- 48 Z. Wang, J. Shin, J. H. Park, H. Lee, D. H. Kim and H. Liu, *Adv. Funct. Mater.*, 2021, **31**, 2008130.
- 49 Y. Shao, Y. Ying and J. Ping, *Chem. Soc. Rev.*, 2020, **49**, 4405–4465.
- 50 E. Bakker, P. Bühlmann and E. Pretsch, *Electroanalysis*, 1999, **11**, 915–933.
- 51 J. Hu, A. Stein and P. Bühlmann, *TrAC, Trends Anal. Chem.*, 2016, **76**, 102–114.
- 52 G. H. Fricke, *Anal. Chem.*, 1980, **52**, 259–275.
- 53 B. Schazmann, D. Morris, C. Slater, S. Beirne, C. Fay, R. Reuveny, N. Moyna and D. Diamond, *Anal. Methods*, 2010, **2**, 342–348.
- 54 A. Abellán-Llobregat, I. Jeerapan, A. Bandodkar, L. Vidal, A. Canals, J. Wang and E. Morallon, *Biosens. Bioelectron.*, 2017, **91**, 885–891.
- 55 J. R. Windmiller, A. J. Bandodkar, G. Valdés-Ramírez, S. Parkhomovsky, A. G. Martinez and J. Wang, *Chem. Commun.*, 2012, **48**, 6794–6796.
- 56 D. Kinnamon, R. Ghanta, K.-C. Lin, S. Muthukumar and S. Prasad, *Sci. Rep.*, 2017, **7**, 1–13.
- 57 H. Y. Y. Nyein, L.-C. Tai, Q. P. Ngo, M. Chao, G. B. Zhang, W. Gao, M. Bariya, J. Bullock, H. Kim and H. M. Fahad, *ACS Sens.*, 2018, **3**, 944–952.
- 58 M. Parrilla, J. Ferré, T. Guinovart and F. J. Andrade, *Electroanalysis*, 2016, **28**, 1267–1275.
- 59 Q. Zhai, L. W. Yap, R. Wang, S. Gong, Z. Guo, Y. Liu, Q. Lyu, J. Wang, G. P. Simon and W. Cheng, *Anal. Chem.*, 2020, **92**, 4647–4655.
- 60 P. R. Miller, X. Xiao, I. Brener, D. B. Burckel, R. Narayan and R. Polsky, *Adv. Healthcare Mater.*, 2014, **3**, 948.
- 61 H. Y. Y. Nyein, W. Gao, Z. Shahpar, S. Emaminejad, S. Challa, K. Chen, H. M. Fahad, L.-C. Tai, H. Ota and R. W. Davis, *ACS Nano*, 2016, **10**, 7216–7224.
- 62 G. Xu, C. Cheng, W. Yuan, Z. Liu, L. Zhu, X. Li, Y. Lu, Z. Chen, J. Liu and Z. Cui, *Sens. Actuators, B*, 2019, **297**, 126743.
- 63 T. Guinovart, M. Parrilla, G. A. Crespo, F. X. Rius and F. J. Andrade, *Analyst*, 2013, **138**, 5208–5215.
- 64 T. Guinovart, A. J. Bandodkar, J. R. Windmiller, F. J. Andrade and J. Wang, *Analyst*, 2013, **138**, 7031–7038.
- 65 A. Pal, V. G. Nadiger, D. Goswami and R. V. Martinez, *Biosens. Bioelectron.*, 2020, **160**, 112206.
- 66 D.-H. Choi, Y. Li, G. R. Cutting and P. C. Searson, *Sens. Actuators, B*, 2017, **250**, 673–678.
- 67 J. Kim, I. Jeerapan, J. R. Sempionatto and A. Bar, *Acc. Chem. Res.*, 2018, **51**, 2820–2828.
- 68 S. Sanei, D. Jarchi and A. G. Constantinides, *Body sensor networking, design and algorithms*, John Wiley & Sons, 2020.
- 69 W. Gao, S. Emaminejad, H. Y. Y. Nyein, S. Challa, K. Chen, A. Peck, H. M. Fahad, H. Ota, H. Shiraki and D. Kiriya, *Nature*, 2016, **529**, 509–514.
- 70 P. M. Farrell, T. B. White, C. L. Ren, S. E. Hempstead, F. Accurso, N. Derichs, M. Howenstine, S. A. McColley, M. Rock and M. Rosenfeld, *J. Pediatr.*, 2017, **181**, S4–S15.
- 71 L. E. Gibson and R. E. Cooke, *Pediatrics*, 1959, **23**, 545–549.
- 72 A. Augarten, S. Hacham, E. Kerem, B. S. Kerem, A. Szeinberg, J. Laufer, R. Doolman, R. Altshuler, H. Blau and L. Bentur, *Pediatr. Pulmonol.*, 1995, **20**, 369–371.
- 73 S. Emaminejad, W. Gao, E. Wu, Z. A. Davies, H. Y. Y. Nyein, S. Challa, S. P. Ryan, H. M. Fahad, K. Chen and Z. Shahpar, *Proc. Natl. Acad. Sci.*, 2017, **114**, 4625–4630.
- 74 J. Gonzalo-Ruiz, R. Mas, C. de Haro, E. Cabruja, R. Camero, M. A. Alonso-Lomillo and F. J. Muñoz, *Biosens. Bioelectron.*, 2009, **24**, 1788–1791.
- 75 M. J. Welsh and B. W. Ramsey, *Am. J. Respir. Crit. Care Med.*, 1998, **157**, S148–S154.
- 76 Z. Sonner, E. Wilder, J. Heikenfeld, G. Kasting, F. Beyette, D. Swaile, F. Sherman, J. Joyce, J. Hagen and N. Kelley-Loughnane, *Biomicrofluidics*, 2015, **9**, 031301.
- 77 S. J. Montain, S. N. Chevront and H. C. Lukaski, *Int. J. Sport Nutr. Exercise Metab.*, 2007, **17**, 574–582.
- 78 J. Kim, G. Valdés-Ramírez, A. J. Bandodkar, W. Jia, A. G. Martinez, J. Ramírez, P. Mercier and J. Wang, *Analyst*, 2014, **139**, 1632–1636.
- 79 W. Jia, A. J. Bandodkar, G. Valdés-Ramírez, J. R. Windmiller, Z. Yang, J. Ramírez, G. Chan and J. Wang, *Anal. Chem.*, 2013, **85**, 6553–6560.
- 80 S. Anastasova, B. Crewther, P. Bembnowicz, V. Curto, H. M. D. Ip, B. Rosa and G.-Z. Yang, *Biosens. Bioelectron.*, 2017, **93**, 139–145.
- 81 D. A. Sakharov, M. U. Shkurnikov, M. Y. Vagin, E. I. Yashina, A. A. Karyakin and A. G. Tonevitsky, *Bull. Exp. Biol. Med.*, 2010, **150**, 83.
- 82 R. A. Robergs, Biochemistry of exercise-induced metabolic acidosis, *Am. J. Physiol.: Regul., Integr. Comp. Physiol.*, 2004, **287**, R502–R516.
- 83 W. He, C. Wang, H. Wang, M. Jian, W. Lu, X. Liang, X. Zhang, F. Yang and Y. Zhang, *Sci. Adv.*, 2019, **5**, eaax0649.
- 84 W. Heng, G. Yang, W. S. Kim and K. Xu, *Bio-Des. Manuf.*, 2021, 1–21.
- 85 L. J. Currano, F. C. Sage, M. Hagedon, L. Hamilton, J. Patrone and K. Gerasopoulos, *Sci. Rep.*, 2018, **8**, 1–11.
- 86 K. Enomoto, R. Shimizu and H. Kudo, *Electron. Commun. Jpn.*, 2018, **101**, 41–46.
- 87 A. M. Zamarayeva, N. A. D. Yamamoto, A. Toor, M. E. Payne, C. Woods, V. I. Pister, Y. Khan, J. W. Evans and A. C. Arias, *APL Mater.*, 2020, **8**, 100905.
- 88 Y. J. Hong, H. Lee, J. Kim, M. Lee, H. J. Choi, T. Hyeon and D. H. Kim, *Adv. Funct. Mater.*, 2018, **28**, 1805754.
- 89 A. E. Von Ah Morano, G. P. Dorneles, A. Peres and F. S. Lira, *J. Cell. Physiol.*, 2020, **235**, 3169–3188.
- 90 F. Hill-Briggs, N. E. Adler, S. A. Berkowitz, M. H. Chin, T. L. Gary-Webb, A. Navas-Acien, P. L. Thornton and D. Haire-Joshu, *Diabetes Care*, 2021, **44**, 258–279.
- 91 B. L. Mealey and G. L. Ocampo, *Periodontology 2000*, 2007, **44**, 127–153.
- 92 B. Piro, G. Mattana and V. Noël, *Sensors*, 2019, **19**, 4376.





- 93 T. D. La Count, A. Jajack, J. Heikenfeld and G. B. Kasting, *J. Pharm. Sci.*, 2019, **108**, 364–371.
- 94 E. V. Karpova, E. V. Shcherbacheva, A. A. Galushin, D. V. Vokhmyanina, E. E. Karyakina and A. A. Karyakin, *Anal. Chem.*, 2019, **91**, 3778–3783.
- 95 J. Kim, J. R. Sempionatto, S. Imani, M. C. Hartel, A. Barfidokht, G. Tang, A. S. Campbell, P. P. Mercier and J. Wang, *Adv. Sci.*, 2018, **5**, 1800880.
- 96 E. Cho, M. Mohammadifar and S. Choi, *IEEE 30th International Conference on Micro Electro Mechanical Systems (MEMS)*, 2017, pp. 366–369, DOI: 10.1109/MEMSYS.2017.7863417.
- 97 W. Han, H. He, L. Zhang, C. Dong, H. Zeng, Y. Dai, L. Xing, Y. Zhang and X. Xue, *ACS Appl. Mater. Interfaces*, 2017, **9**, 29526–29537.
- 98 A. Martín, J. Kim, J. F. Kurniawan, J. R. Sempionatto, J. R. Moreto, G. Tang, A. S. Campbell, A. Shin, M. Y. Lee and X. Liu, *ACS Sens.*, 2017, **2**, 1860–1868.
- 99 A. Dos Santos, E. Fortunato, R. Martins, H. Águas and R. Igreja, *Sensors*, 2020, **20**, 4407.
- 100 M. L. Hammock, A. Chortos, B. C. K. Tee, J. B. H. Tok and Z. Bao, *Adv. Mater.*, 2013, **25**, 5997–6038.
- 101 Z. Lou, L. Wang and G. Shen, *Adv. Mater. Technol.*, 2018, **3**, 1800444.
- 102 M. A. Nystoriak and A. Bhatnagar, *Front. Cardiovasc. Med.*, 2018, **5**, 135.
- 103 R. H. Fagard, *J. Hum. Hypertens.*, 2005, **19**, S20–S24.
- 104 J. R. MacDonald, *J. Hum. Hypertens.*, 2002, **16**, 225–236.
- 105 A. Crisafulli, F. Tocco, G. Pittau, L. Lorrari, C. Porru, E. Salis, P. Pagliaro, F. Melis and A. Concu, *Appl. Physiol., Nutr., Metab.*, 2006, **31**, 423–431.
- 106 P. Kokkinos, *Hypertension*, 2014, **64**, 1160–1164.
- 107 X. P. A. Gao, G. Zheng and C. M. Lieber, *Nano Lett.*, 2010, **10**, 547–552.
- 108 S. Jung, T. Ji and V. K. Varadan, *Appl. Phys. Lett.*, 2007, **90**, 062105.
- 109 I. Graz, M. Kaltenbrunner, C. Keplinger, R. Schwödiauer, S. Bauer, S. P. Lacour and S. Wagner, *Appl. Phys. Lett.*, 2006, **89**, 073501.
- 110 C. Pang, G.-Y. Lee, T.-i. Kim, S. M. Kim, H. N. Kim, S.-H. Ahn and K.-Y. Suh, *Nat. Mater.*, 2012, **11**, 795–801.
- 111 S. C. B. Mannsfeld, B. C. K. Tee, R. M. Stoltenberg, C. V. H. H. Chen, S. Barman, B. V. O. Muir, A. N. Sokolov, C. Reese and Z. Bao, *Nat. Mater.*, 2010, **9**, 859–864.
- 112 M. B. Haddad, T. W. Wilson, K. Ijaz, S. M. Marks and M. Moore, *Jama*, 2005, **293**, 2762–2766.
- 113 B. A. Sheikh, B. A. Bhat, U. Mehraj, W. Mir, S. Hamadani and M. A. Mir, *Curr. Pharm. Biotechnol.*, 2021, **22**, 480–500.
- 114 T. R. Frieden, P. I. Fujiwara, R. M. Washko and M. A. Hamburg, *N. Engl. J. Med.*, 1995, **333**, 229–233.
- 115 N. R. Gandhi, P. Nunn, K. Dheda, H. S. Schaaf, M. Zignol, D. Van Soolingen, P. Jensen and J. Bayona, *Lancet*, 2010, **375**, 1830–1843.
- 116 C. P. Chaulk and V. A. Kazandjian, *Jama*, 1998, **279**, 943–948.
- 117 M. C. Raviglione, *Tuberculosis*, 2003, **83**, 4–14.
- 118 T. R. Frieden and J. A. Sbarbaro, *Bull. W. H. O.*, 2007, **85**, 407–409.
- 119 O. World Health, *Global tuberculosis report 2013*, World Health Organization, 2013.
- 120 Y. Feleke, J. Abdulkadir and G. Aderaye, *East Afr. Med. J.*, 1999, **76**, 361–364.
- 121 O. O. Adewole, G. E. Erhabor, T. O. Adewole, A. O. Ojo, H. Oshokoya, L. M. Wolfe and J. E. Prenni, *Proteomics: Clin. Appl.*, 2016, **10**, 547–553.
- 122 M. J. Patterson, S. D. R. Galloway and M. A. Nimmo, *Exp. Physiol.*, 2000, **85**, 869–875.
- 123 H. Lee, C. Song, Y. S. Hong, M. S. Kim, H. R. Cho, T. Kang, K. Shin, S. H. Choi, T. Hyeon and D.-H. Kim, *Sci. Adv.*, 2017, **3**, e1601314.
- 124 J. R. Sempionatto, M. Lin, L. Yin, E. De la paz, K. Pei, T. Sonsard, A. N. d. L. Silva, A. A. Khorshed, F. Zhang, N. Tostado, S. Xu and J. Wang, *Nat. Biomed. Eng.*, 2021, **5**, 737–748.

